THE JOURNAL OF BIOLOGICAL CHEMISTRY VOL. 289, NO. 15, pp. 10502–10509, April 11, 2014
Published in the U.S.A.

Structural Basis for Inactivation of *Giardia lamblia* Carbamate Kinase by Disulfiram*

Received for publication, January 27, 2014, and in revised form, February 12, 2014 Published, JBC Papers in Press, February 20, 2014, DOI 10.1074/jbc.M114.553123

Andrey Galkin[‡1], Liudmila Kulakova[‡1], Kap Lim[‡1], Catherine Z. Chen[§], Wei Zheng[§], Illarion V. Turko[‡¶], and Osnat Herzberg[‡‖2]

From the [‡]Institute for Bioscience and Biotechnology Research, University of Maryland, Rockville, Maryland 20850, [§]Therapeutics for Rare and Neglected Diseases, National Center for Advancing Translational Sciences, National Institutes of Health, Bethesda, Maryland 20892, the [¶]National Institute of Standards and Technology, Gaithersburg, Maryland 20899, and the [‖]Department of Chemistry and Biochemistry, University of Maryland, College Park, Maryland 20742

Background: Carbamate kinase is an essential *Giardia lamblia* enzyme, and the anti-alcoholism drug disulfiram kills the trophozoites and inhibits the enzyme.
Results: Disulfiram acts by modifying Cys-242 adjacent to the active site and cures giardiasis in mice.
Conclusion: *G. lamblia* CK is a good drug target and disulfiram may be repurposed as antigiardiasis drug.
Significance: We need new antigiardiasis drugs because current treatments fail frequently.

Carbamate kinase from *Giardia lamblia* is an essential enzyme for the survival of the organism. The enzyme catalyzes the final step in the arginine dihydrolase pathway converting ADP and carbamoyl phosphate to ATP and carbamate. We previously reported that disulfiram, a drug used to treat chronic alcoholism, inhibits *G. lamblia* CK and kills *G. lamblia* trophozoites *in vitro* at submicromolar IC_{50} values. Here, we examine the structural basis for *G. lamblia* CK inhibition of disulfiram and its analog, thiram, their activities against both metronidazole-susceptible and metronidazole-resistant *G. lamblia* isolates, and their efficacy in a mouse model of giardiasis. The crystal structure of *G. lamblia* CK soaked with disulfiram revealed that the compound thiocarbamoylated Cys-242, a residue located at the edge of the active site. The modified Cys-242 prevents a conformational transition of a loop adjacent to the ADP/ATP binding site, which is required for the stacking of Tyr-245 side chain against the adenine moiety, an interaction seen in the structure of *G. lamblia* CK in complex with AMP-PNP. Mass spectrometry coupled with trypsin digestion confirmed the selective covalent thiocarbamoylation of Cys-242 in solution. The *Giardia* viability studies in the metronidazole-resistant strain and the *G. lamblia* CK irreversible inactivation mechanism show that the thiuram compounds can circumvent the resistance mechanism that renders metronidazole ineffectiveness in drug resistance cases of giardiasis. Together, the studies suggest that *G. lamblia* CK is an attractive drug target for development of novel antigiardial therapies and that disulfiram, an FDA-approved drug, is a promising candidate for drug repurposing.

The enteric protozoan, *Giardia lamblia*, causes the human intestinal disease giardiasis, a severe diarrheal disease commonly acquired from contaminated freshwater and public water supplies and by a direct fecal-oral route. Giardiasis is highly prevalent in the developing world with the latest estimates of 280 million infected people worldwide (1). The infective *Giardia* cysts are not destroyed by chemical treatment of public water sources; thus, the disease is difficult to control in poor countries lacking adequate water management. Reinfection reaches as high as 90% in regions where infection is highly endemic and where environmental contamination is high. Moreover, treatment failures with standard care drugs such as metronidazole, tinidazole, and albendazole occur at ~20% rate (2–6). Giardiasis has negative economical impact in underdeveloped and developing countries. In particular, chronically infected children suffer from malnutrition, growth retardation, poor cognitive function, and death. The spread of strains resistant to currently available drugs is a growing concern, and the unpleasant side effects of these drugs lead to non-compliance. Finally, prevention of infections through vaccines has proven a challenge because *G. lamblia* evade the host immune system by displaying variant-specific surface proteins. Clearly, there is a need for new alternative anti-giardia drugs that are not subjects to current resistance mechanisms.

G. lamblia utilizes the arginine dihydrolase pathway to produce ATP from ADP and L-arginine (7), a pathway that is absent in high eukaryotes, including humans. The arginine dihydrolase pathway employs three enzymes, arginine deiminase, ornithine transcarbamoylase, and carbamate kinase (CK;[3] EC 2.7.2.2). CK catalyzes the last step of the pathway, converting carbamoyl phosphate and ADP into carbamate and ATP. We have shown that the enzyme from *G. lamblia* (*G. lamblia* CK) is essential for the survival of the trophozoites, and determined three crystal structures of the enzyme, one in complex with the non-hydrolysable ATP analog, AMP-PNP, the second with a

* This work was supported by the National Institutes of Health Grant R56AI059733 (to O. H.) and Science Applications International Corporation/NCI, National Institutes of Health contract 11XS049 (to O. H.), and the Intramural Research Programs of the Therapeutics for Rare and Neglected Diseases, National Center for Advancing Translational Sciences, National Institutes of Health (to C. Z. C. and W. Z.).
The atomic coordinates and structure factors (code 4OLC) have been deposited in the Protein Data Bank (http://wwpdb.org/).
[1] These authors contributed equally to this work.
[2] To whom correspondence should be addressed: Institute for Bioscience and Biotechnology, University of Maryland, 9600 Gudelsky Dr., Rockville, MD 20850. Tel.: 240-314-6245; Fax: 240-314-6255; E-mail: osnat@umd.edu.

[3] The abbreviations used are: CK, carbamate kinase; MLC, minimum lethal concentration; AMP-PNP, γ-imino-ATP.

carbamate phosphate analog, citric acid, and the third in the unbound state (8, 9). These structures revealed several modes of enzyme conformational flexibility.

The essentiality of *G. lamblia* CK, the absence of the enzyme in the human genome, and the ample precedence of "druggablility" of kinases, have led us to target *G. lamblia* CK for drug development. To enable high throughput compound library screening, we have developed two bioluminescence-based assays that monitor ATP production. One assay monitors the cellular ATP content, which correlates with the viability of *G. lamblia* trophozoites, and the second assay measures the ATP produced by the *G. lamblia* CK reaction. We used these assays to identify compounds that both kill the organism and inhibit *G. lamblia* CK. We screened the LOPAC^{1280} library of pharmaceutical active compounds and the NIH Chemical Genomics Center Pharmaceutical Collection library of approved drugs (10, 11). Disulfiram (tetraethylthiuram disulfide) was found the most potent compound that inhibited *G. lamblia* CK (IC_{50} = 0.58 μM) and killed the *Giardia* trophozoites (IC_{50}, 0.9 μM), while exhibiting no toxicity in HepG2 mammalian cells at the highest employed concentration (40 μM).

Disulfiram, also known as antabuse, is a commonly used drug for long term treatment of chronic alcoholism. The drug inhibits its acetaldehyde dehydrogenase by specifically modifying one of the active site cysteine residues of the enzyme. The cysteine modification is followed by elimination and formation of a disulfide bond between two active site cysteine residues (12, 13). Enzyme inactivation leads to an aversive reaction to alcohol consumption (severe hangover-like symptoms), which is avoided by abstaining from alcohol. Although disulfiram contains a thiocarbamate group that can potentially interacts with multiple targets, studies have concluded that the drug has an acceptable side effect profile for long term treatments of alcoholism at the daily doses of 250–500 mg (14, 15). Because disulfiram has been identified as the first submicromolar inhibitor of *G. lamblia* CK as well as a compound that kills *Giardia* trophozoites, we have undertaken structural and mass spectrometry studies to characterize the enzyme/inhibitor complex.

A previous potential antigiardiasis drug search using compounds known to bind to zinc finger proteins discovered that disulfiram was effective against *Giardiasis* in adult mice but did not identify the molecular target (16). Through the above two high throughput screening assays, we have independently identified disulfiram as a *Giardia*-cidal compound that acts through the essential *G. lamblia* CK enzyme (10, 11). We also validated the result *in vivo* using an improved adult mouse model that enables quantitative determination of the reduced trophozoite load by coupling the drug treatment to *in vitro* proliferation assay of axenic *G. lamblia* GS cultures. Here, we report the results of the structural and *in vivo* studies.

EXPERIMENTAL PROCEDURES

Protein Preparation, Crystallization, and Structure Determination—Pure *G. lamblia* CK was produced as described previously (8). The purified protein was concentrated to 30 mg/ml in solution containing 50 mM Tris-HCl, pH 8.0, 0.1 M NaCl, 5 mM $MgCl_2$, and 1 mM DTT (dithiothreitol) and stored in aliquots at −80 °C.

Crystals of *G. lamblia* CK were grown at room temperature by the vapor diffusion methods in hanging drops. The reservoir solutions contained 0.4 M ammonium citrate dibasic, pH 5.0, and 21% PEG 3350. The hanging drops consisted of 1:1 protein and reservoir solutions. This condition yielded the structure of *G. lamblia* CK with bound citric acid (9). 100 mM disulfiram (Sigma-Aldrich) dissolved in dimethyl sulfoxide was diluted in mother liquor to a final concentration of 2 mM. Crystals were soaked in this drug solution for 16 h and then transferred to mother liquor containing 20% glycerol and flash-cooled in liquid nitrogen for x-ray diffraction data acquisition.

X-ray diffraction data were collected at the GM/CA-CAT synchrotron beamline 23ID at the Advanced Photon Source in Argonne National Laboratory (Argonne, IL). The beamline was equipped with the MARmosaic 300 CCD detector (Marresearch GmbH) controlled with the JBluIce user interface program.

Diffraction data were integrated with the XDS program (17) and scaled with the AIMLESS program, the successor to SCALA (18), as implemented in CCP4 (19). The initial structure was determined by Furrier synthesis using the coordinates and calculated phases of the previously determined protein structure (9). Rigid body minimizations and refinements were carried out with the Phenix program (20). A fragment of the disulfiram crystal structure coordinates (21) was added to a modified cysteine residue seen in the electron density map. The Coot graphics program (22) was used for model building and visual inspection of the structures. Structure figures were generated with Raster3D linked to Molscript (23, 24) and PyMOL (DeLano Scientific).

Mass Spectrometry—Mass spectrometry (MS) analysis coupled with trypsin digestion was performed to identify residues modified by disulfiram in solution. The *G. lamblia* CK was mixed with disulfiram at 1:150 molar ratio in 50 mM NH_4HCO_3 buffer (pH 7.7). The sample was treated with trypsin (Sigma-Aldrich) at 1:25 (w/w) enzyme/substrate ratio for 14 h at 37 °C. Following proteolysis, the protein sample was treated with 50 mM iodoacetamide for 60 min at room temperature. Aliquots of the sample were then mixed with equal volumes of 10 mg/ml α-cyano-4-hydroxycinnamic acid dissolved in 50% acetonitrile and 0.1% trifluoroacetic acid. The MS analysis was performed with an AB4700 Proteomics Analyzer (Applied Biosystems, Framingham, MA).

The MS mode acquisitions consisted of 1,000 laser shots averaged over 20 sample positions. For MS/MS mode acquisitions, 3,000 laser shots were averaged over 30 sample positions for post source decay fragments. Combined acquisition of MS and MS/MS data were automatically controlled with the 4000 Series Explorer software (version 3.0). Data analysis was performed with the GPS Explorer software utilizing Mascot (MatrixScience, version 2.0, London, UK) as the search engine. During the search, the mass tolerance was 0.08 Da for the precursor ions and 0.2 Da for the fragment ions.

G. lamblia Cultures—Trophozoites of *G. lamblia* Assemblage A isolate WB, Assemblage B isolate GS/H7 (25), and Assemblage A metronidazole-resistant isolate 713M3 (26) were grown anaerobically in borosilicate glass screw-cap culture tubes (Thermo Fisher) at pH 7.0 in modified TYI-S-33 medium

(11, 27). The medium was supplemented with 10% heat-inactivated bovine serum (Sigma-Aldrich) and 0.05% bovine bile (Sigma-Aldrich). To attain low-oxygen-tension conditions, the tubes were filled to 85 to 90% of their total volume capacity and incubated without shaking at 37 °C. Subcultures (2×10^5 trophozoites per tube) were made three times a week. For enumeration and for mouse infection, the trophozoites were detached from the wall of the tube by chilling the cultures on ice for 20 min.

Minimum Lethal Concentration (MLC) Determination—MLC values were determined by incubating *G. lamblia* trophozoites with the drugs in 96-well culture plates (Corning, Inc.), followed by transferring the trophozoites into 8-ml tubes (Fisher Scientific) for proliferation. Assays were performed in duplicates. Dry compounds were dissolved in dimethyl sulfoxide (Sigma) at stock concentration of 10 mM and then diluted 1:100 fold in growth medium to a final compound concentration of 100 μM. 100-μl aliquots of compound solutions were prepared by 2-fold serial dilutions (12 concentrations) in medium. This was followed by the addition of 10 μl of *G. lamblia* culture containing 10,000 organisms into medium with the compound to be tested. All growth medium used contained reduced cysteine concentration (2.9 mM cysteine) because the usual concentration (11.6 mM) blunts the activities of thiuram compounds (16). Metronidazole mixed with the same medium served as positive control, and the medium with dimethyl sulfoxide alone served as negative control. Plates were incubated under anaerobic condition in sealed bags (Becton Dickinson and Company) at 37 °C for 3 days and surveyed visually under the microscope to check trophozoite survival, mobility, and attachment. The plates were chilled on ice for 30 min, and the entire contents of each of 4 wells in the growth/death transition were transferred into the 8-ml tubes containing growth medium and no drug. The tubes were incubated under anaerobic condition for 3 days at 37 °C and checked under microscope. The MLC value was attributed to the lowest concentration without any live organisms.

ATP Content Assay—The ATP content assay was described in detail previously (11). The assays were performed in duplicates. Tubes containing *G. lamblia* trophozoites were placed on ice for 30 min. 100-μl aliquots of each tube were transferred into 96-well black clear-bottom assay plate followed by the addition of 70 μl/well of the ATPLite reagent (PerkinElmer Life Science) to initiate a one-step cell lysis and detection of the ATP level. The luminescence signals were measured on an EnSpire 2300 plate reader (PerkinElmer Life Science).

Giardiasis Animal Model and Drug Treatment—Fifteen adult (4-week-old) C57BL/6J female mice (The Jackson Laboratory, Bar Harbor, ME) were infected with *G. lamblia* GS/H7 trophozoites, the only human *Giardia* isolate known to infect adult mice (28). The trophozoites (500,000 suspended in 200 μl of TYI-S-33 medium) were administered by oral gavage. On days 3 through 6 after infection, five mice were treated once daily with 5 mg of disulfiram (or dithiodimethylthiuram), whereas the remaining untreated five mice served as control. A comparison experiment with metronidazole was carried out with 15 mice, treating 10 animals and leaving five animals untreated for control. The drugs were suspended in 200 μl of corn oil and were administered by oral gavage. All mice were euthanized on day 7. Two inches of the upper small intestine were dissected and washed with 2 ml of medium supplemented with antibiotics (piperacillin 1 mg/ml, moxalactam 1 mg/ml). The harvested small intestines were opened longitudinally and minced in a Petri dish containing 10 ml of ice-chilled medium. Plates were placed on ice for 30 min to allow the trophozoites to detach from the intestine and were surveyed under microscope for estimation of trophozoites population by the plate survey method described previously (16). The trophozoites were enumerated in several random fields at all depths not obscured by intestines at a magnification of 20× with an Axiovert 40 C microscope (Zeiss). The University of Maryland College Park The Institutional Animal Care and Use Committee approved the animal studies.

Mouse Trophozoite Load Quantification by Proliferation of Axenic Cultures—The entire contents of each Petri dish was transferred into a 15-ml glass tube, the volume was adjusted to 14 ml by adding medium containing 1 mg/ml piperacillin and 1 mg/ml moxalactam, and the tube was vigorously vortexed to separate the trophozoites from the intestine debris. For the following 2 h, tubes were kept at 37 °C to allow trophozoite attachment to the wall of the glass tube, after which the medium containing the intestine debris was decanted and replaced by fresh medium. Tubes were kept at 37 °C for another 15 min followed by a second medium replacement, but this time the medium was supplemented with 1 mg/ml piperacillin, 1 mg/ml moxalactam, 5 μg/ml amoxicillin/clavulanic acid, and 10 μg/ml nalidixic acid. The tubes were kept at 37 °C for 6 days for proliferation. Trophozoites growth was determined once daily by direct cell counting using a Beckman Coulter Z1 counter (Beckman Coulter, Inc.) and by monitoring the ATP content using the ATPLite reagent.

The proliferation measurements were used to calculate growth curves and trophozoite load of drug-treated mice compared with untreated mice. Trophozoite load was quantified by calculating the initial population from the growth curves, fitting the luminescence or the trophozoite counting data to the Malthusian model of exponential growth $N_t = N_0 e^{rt}$, where N_t is the signal of the population at time t, r is the growth rate, and N_0 is the value we seek to determine, the signal of the initial population at the end of treatment. The % load was determined relative to N_0 of untreated mouse samples. The two methods of measurement yielded consistent results.

RESULTS AND DISCUSSION

Disulfiram Impairs the Viability of Metronidazole-susceptible and Metronidazole-resistant G. lamblia Isolates—The bioluminescence assay that measures the cellular ATP content is a cell viability assay amenable to high throughput screening of compound libraries. However, this assay does not discriminate between cell killing and metabolically inactive trophozoites. In contrast, MLC assays, first incubating the trophozoites with the drug and then transferring the culture to drug-free medium for proliferation, determine the drug concentration when no surviving organisms remain. MLC values were determined for disulfiram and thiram using three *G. lamblia* isolates that infect human: the metronidazole-susceptible WB and GS/H7, and the

metronidazole-resistant 713M3. The data are summarized in Table 1 together with the *G. lamblia* CK IC_{50} values, confirming the potency of disulfiram and thiram against both metronidazole-susceptible and metronidazole-resistant isolates. Hence, these compounds and possibly future *G. lamblia* CK inhibitors would not be subject to the metronidazole resistance mechanism, supporting the hypothesis that *G. lamblia* CK is a novel target for the development of new antigiardiasis drugs.

Disulfiram Interferes with Nucleotide Binding by Covalently Modifying Cys-242—Recently, we have reported the crystal structures of *G. lamblia* CK in complexes with the non-hydrolysable ATP analog AMP-PNP and with citric acid, which mimics carbamoyl phosphate binding (8, 9). These structures reveal how the phosphoryl group transfer occurs and provide the structural basis for understanding how disulfiram inhibits enzyme activity. Briefly, elongated active site architecture enables the accommodation of the two substrates, ADP and carbamoyl phosphate, in line for direct transfer of the phosphoryl group to produce ATP and carbamate. Superposition of the two enzyme-ligand structures shows that the binding site of the AMP-PNP γ-phosphoryl group overlaps with a carboxylate group of the citrate, the surrogate of the carbamoyl phosphate phosphoryl group. An auxiliary domain encompassing amino acid residues 134–164 adopts a closed conformation when the citric acid binds (Fig. 1*A*) but adopts an open or disordered conformation when AMP-PNP binds and displaces the citric acid (Fig. 1*B*). Another region of enzyme flexibility, located at the nucleotide binding site, comprises a loop carrying Tyr-245 (amino acid residues 244–250). The loop adjusts upon nucleotide binding such that the aromatic ring of the tyrosine stacks above the adenine group (Fig. 1*B*). In contrast, in the absence of nucleotide the loop either lacks well defined conformation, or it adopts an open conformation that places Tyr-245 more remotely from the adenine site (Fig. 1*A*).

The crystal structure of *G. lamblia* CK soaked with disulfiram was determined to the resolution limit of 2.6 Å. Data collection and refinement statistics are summarized in Table 2.

TABLE 1

Inhibition of *G. lamblia* CK activity and growth of *G. lamblia* isolates by drugs

Compound	CK IC_{50}[a]	*G. lamblia* MLC[b]		
		WB	GS/H7	713M3
	μM		μM	
Disulfiram	0.64	3.1	1.5	0.75
Thiram	0.15	0.75	0.8	0.38
Metronidazole	Not inhibited	3.1	3.1	50

[a] Values were reported previously (10).
[b] Values for all three compounds were determined with medium containing 2.9 mM cysteine rather than the usual 11.6 mM included in optimal laboratory medium to prevent masking of the activity of thiuram compounds.

TABLE 2

X-ray data collection and structure refinement statistics

r.m.s.d., root mean square deviation.

Data collection	
Space group	$P2_1$
Cell dimension	$a = 70.3$, $b = 98.2$, and $c = 102.7$ Å, $\beta = 107.6°$
Wavelength (Å)	1.0332
Resolution (Å)	2.6
No. of observed reflections	137,419
Completeness (%)[a]	99.1 (99.7)
No. of unique reflections	40,662
R_{merge}[b]	0.082 (0.314)
$\langle I/\sigma(I)\rangle$	10.8 (3.8)
Redundancy	3.4 (3.4)
Refinement	
No. of reflections used	40,453
No. of protein atoms	9,168
No. of ligand atoms	76
No. of water atoms	265
R_{cryst}[c]	0.199 (0.232)
R_{free}[d]	0.265 (0.320)
r.m.s.d. from ideal geometry	
Bond length (Å)	0.009
Bond angle	1.2°
Average B factor (Å^2)	
Protein	43
Ligand	65
Water	36
Ramachandran plot (%)[e]	86.9, 13.1, 0.0, 0.0

[a] The values in parentheses are for the highest resolution shell, 2.71–2.60 Å.
[b] $R_{merge} = \Sigma_{hkl}[(\Sigma_j|I_j - \langle I\rangle|)/\Sigma_j|I_j|]$.
[c] $R_{cryst} = \Sigma_{hkl}||F_o| - |F_c||/\Sigma_{hkl}|F_o|$, where F_o and F_c are the observed and calculated structure factors, respectively.
[d] R_{free} is computed with 2,013 randomly selected reflections omitted from the refinement.
[e] Ramachandran plot categories are most favored, allowed, generously allowed, and disallowed (32, 33).

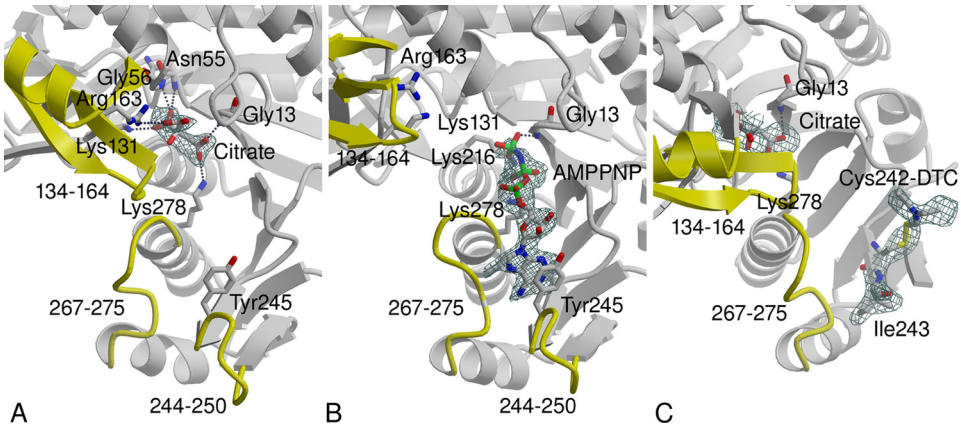

FIGURE 1. **Difference Fourier electron density maps associated with ligands bound in the active site of *G. lamblia* CK: the coefficients $F_o - F_c$ and calculated phases omitting the ligands from the calculation are used.** *A*, citric acid bound in the carbamoyl phosphate binding site. *B*, AMP-PNP bound in the ADP/ATP binding site. *C*, the disulfiram thiocarbanoylation product modifying Cys-242 adjacent to the ADP/ATP binding site and the citric acid in the carbamoyl phosphate binding site. Atomic colors are as follows: *gray*, carbon; *red*, oxygen; *blue*, nitrogen; and *green*, phosphor. Active site regions that undergo conformational transitions are highlighted in *yellow*, and their amino acid residue ranges are labeled. The 244–250 loop is disordered in *C*. *A* and *B* are adopted from Ref. 9.

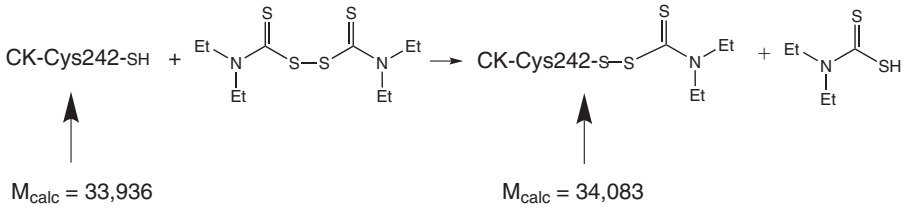

FIGURE 2. **The proposed thiocarbamoylation reactions leading to the modification of Cys-242.**

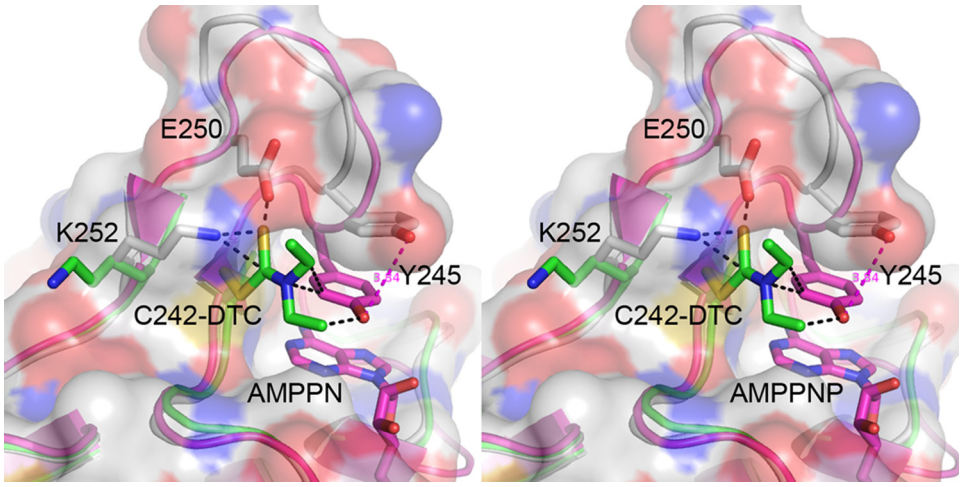

FIGURE 3. **Stereoscopic representation of the environment of Cys-242 superposed in three conformational states.** The AMP-PNP bound structure (*magenta*), the citric acid bound structure (*gray*), and the thiocarbamoylated structure, which exhibits disordered 244–250 loop (*green*). The 3.8 Å shift of the Tyr-245 side chain in response to AMP-PNP binding is highlighted by the *magenta dashed line*. Steric clashes contacts between the modified Cys-242 and other side chains are indicated by *black dashed lines*. The transparent protein surface corresponds to the citric acid bound structure.

The disulfiram reacted with a single *G. lamblia* CK cysteine residue, Cys-242, to form a covalent product seen in one of the four subunits in the crystal asymmetric unit. The electron density map is consistent with a thiodiethylcarbamoyl adduct, which suggests the dithiocarbamoylation reaction depicted in Fig. 2, except that there is no electron density to account for the sulfur of thioketone (Fig. 1*C*). The degradation of the dithiodiethylcarbamoyl adduct into thiodiethylcarbamoyl adduct may be attributed to radiation damage during x-ray data collection. X-ray radiation, in particular high-energy synchrotron radiation, has long been known to cause disulfide bond breakage and decarboxylation of acidic side chains in protein crystals, even at cryogenic temperature (29, 30). A modified Cys-242 contains a disulfide bond and a thioketone, both prone to radiation damage. Although missing in the electron density map, the position of the thioketone sulfur is defined by the stereochemistry, as depicted in the model shown in Fig. 3. Note that the electron density map shows thiocarbamoylation of only one of four of the *G. lamblia* CK Cys-242 in the crystal asymmetric unit. The data cannot distinguish between cleavage of the thiocarbamate group by the x-ray radiation and an unmodified thiol group. Interestingly, in addition to the covalently linked thiocarbamoyl adduct, the electron density map contained two extensive peaks ~11 Å away from two free Cys-242 residues, which were modeled as free dithiodiethylcarbamate molecules that may account for degradation of other modified cysteine residues. As described below, the mass spectrometry studies confirmed that disulfiram selectively modifies the majority of the Cys-242 thiol groups.

Modification of Cys-242 interferes with the conformational transition that accompanies nucleotide binding, whereas the citric acid binding remains unaltered and the auxiliary domain is in the closed conformation. The affected region is shown in Fig. 3, which depicts the superposition of the 244–250 loop environment in the absence and presence of nucleotide (*gray* and *magenta*, respectively), and in the presence of the thiocarbamoylated Cys-242 (*green*). In the absence of AMP-PNP, the Cys-242 thiol group interacts with Lys-252 amino group (3.5 Å), which in turn, forms a salt bridge with Glu-250. Upon nucleotide binding the loop undergoes adjustments that bring Cys-242 closer to Glu-250 (3.0 Å). Thus, the Cys-242-Glu-250-Lys-252 triad plays crucial role in defining the loop conformational adjustments and the correlated 3.8 Å shift of Tyr-245 (Fig. 3). Dithiocarbamoylation of Cys-242 leads to steric clashes with both Glu-250 and Lys-252 side chains. To avoid these clashes, Lys-252 backbone flips concomitantly with disordering of the 244–250 loop. Moreover, the position of the modified Cys-242 overlaps with Tyr-245 side chain at the ATP-PNP bound state. Thus, the crystal structure is consistent with inhibition mechanism due to irreversible modification of Cys-242 that prevents nucleotide binding.

The mass spectrometry analysis confirmed that disulfiram modified the Cys-242 thiol, selectively. The enzyme contains eight cysteine residues, three of which are exposed to solvent and only Cys-242 is located in the vicinity of the active site. MALDI-TOF analysis showed that mixing *G. lamblia* CK with 150-fold molar excess of disulfiram yielded a single molecular peak shifted by 151 mass units relative to the untreated protein

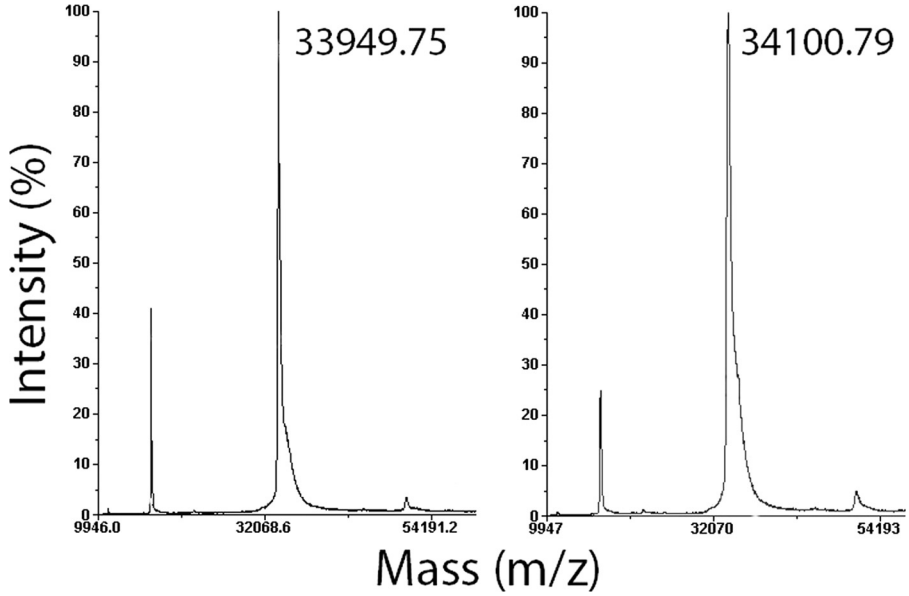

FIGURE 4. **MALDI-TOF mass spectroscopy of *G. lamblia* CK before (*left panel*) and after (*right panel*) addition of disulfiram.** The small discrepancies between the calculated molecular masses (see Fig. 2) and those measured by mass spectrometry are well within the experimental error. The mass difference of 151 units is consistent with a single cysteine modified by a dithiodiethylcarbamate group (calculated mass difference of 148 units).

TABLE 3

***In vivo* mice studies of trophozoite load following disulfiram, thiram, and metronidazole treatments (once daily dose of 5 mg/day for 4 days)**

	Trophozoite load, *p* value[a]		
		Proliferation assay[b]	
Drug	Visual plate survey	Trophozoite count	ATP content
		%	
Disulfiram	1.2 (0.004)	0.45 ± 1.01 (0.0032)	0.55 ± 0.97 (0.00037)
Thiram	0.4 (0.004)	0.± 0. (0.0032)	0.04 ± 0.08 (0.00038)
Metronidazole	1.9 (0.003)	0.01 ± 0.02 (0.00023)	0.002 ± 0.0052 (0.000006)

[a] Trophozoite load is calculated relative to the untreated mice. The *p* value is calculated based on a t-test relative to the trophozoite load of the control untreated mice.
[b] The trophozoite load calculated from the growth curves at time 0, *i.e.* the end of animal treatment, either by cell counting or ATP luminescence (see "Experimental Procedures" for detail).

peak (Fig. 4). This mass difference is consistent with a single cysteine modification by a dithiodiethylcarbamate group that should increase the protein mass by 148 units. Trypsin digestion followed by MS/MS mass spectrometry analysis identified the Cys-242-containing peptide as the sole dithiocarbamoylated peptide. Thus, both the crystal structure and mass spectrometry in solution suggest that Cys-242 thiol group is the most reactive of all *G. lamblia* CK thiol groups. The electrostatic microenvironment of the Cys-242, including the Glu-250-Lys-252 pair, may enhance the reactivity of this thiol group.

Adult Mouse Model and Culture Axenization—The human *G. lamblia* GS/H7 is the only known isolate that also infects adult mice. Other human isolates infect neonatal mice, which are more delicate and prone to accidental injuries during oral gavage. We therefore elected to evaluate the efficacy of antigiardiasis compounds in adult mice infected with *G. lamblia* GS/H7 trophozoites. Of the sources of C57BL/6J mice tested, only mice from The Jackson Laboratory were consistently infected, and after a week (corresponding to the entire period of the *in vivo* infection and drug treatment experiments), the trophozoite population could be enumerated using a plate survey method (16). However, following drug treatment the remaining trophozoites were too few for reliable estimation. To quantify determine parasite survival, the *in vivo* studies were followed by *in vitro* proliferation assays.

Because the gut flora is populated by anaerobic bacterial species that thrive on the medium required for *in vitro* optimal anaerobic trophozoite growth, obtaining axenic *G. lamblia* cultures reproducibly is crucial for the proliferation experiments. Recently, axenization of *Giardia* cultures harvested from the intestines of suckling mice has been reported (31). The published method consists of harvesting the intestine of the treated mice and transferring the luminal washes to the peritoneal cavity of adult mice for 24 h and then euthanizing these mice to obtain the intraperitoneal content used in the *in vitro* proliferation assay. We have developed a simpler axenization method that avoids the doubling of sacrificed mice by identifying an antibiotic mixture that does not interfere with *G. lamblia* growth. This mixture includes the standard antibiotics used to avoid bacterial contamination in *in vitro* studies (piperacillin and moxalactam) as well as the combination drug amoxicillin/clavulanic acid and the quinolone nalidixic acid. We have used this mouse model and axenization protocol extensively for two years and rarely encountered bacterial contamination. The requirement for clavulanic acid, a class A β-lactamase inhibitor, suggests that the commensal bacteria in the gut of The Jackson Laboratory C57BL/6J mice have acquired this enzyme, not a

surprising finding considering the wide use of β-lactam antibiotics. In case of emergence of new antibiotic resistance in commensal bacteria, alternative inhibitors may be identified that enable axenization of the *in vitro G. lamblia* cultures.

Disulfiram and Thiram Cure Giardiasis in Adult Mice—Previously, Nash and Rice (16) reported cure or reduced *Giardia* trophozoite load in adult mice treated daily with 25-mg disulfiram doses for 4 days. We reduced the doses to 5 mg/day and observed comparable drug efficacies of disulfiram, thiram, and metronidazole, in contrast to the untreated mice that remained infected (Table 3). For all three drugs, trophozoites could not be detected in most mice, and only a few trophozoites could be detected in 20–40% of the treated mice. Moreover, both proliferation quantification methods (direct trophozoite count and ATP content determination) yielded similar results. Thus, these experiments demonstrate that disulfiram, an FDA-approved drug, is a potential antigiardiasis therapeutic agent. (Thiram is not an approved drug.) Further dose and schedule studies in animals followed by human clinical studies will be necessary to validate the effectiveness of disulfiram treatment.

Future Prospects—The arginine dihydrolase pathway enzyme, CK, is essential for *G. lamblia* trophozoite survival, and the enzyme is irreversibly inactivated by disulfiram and its analog, thiram. These compounds kill metronidazole-susceptible and metronidazole-resistant *G. lamblia* trophozoites *in vitro* and exhibit efficacy *in vivo* in mouse model. CK has not been exploited as antigiardial drug target; thus, future inhibitors will not be subject to drug resistance mechanisms against current standard care drugs. Unlike treatment of chronic alcoholism, which requires long term use of the drug, antigiardiasis therapy is expected to span only a short period, reducing the risk of side effects. Nevertheless, compound modification that increases selectivity toward *G. lamblia* CK would avoid undesirable side effects due to off target inhibition of the human acetaldehyde dehydrogenase. Improved selectivity and potency may be achieved if one of the ethyl substituents is replaced by a larger group that occupies more of the adenine binding site. Moreover, *G. lamblia* trophozoites attach to the wall of the intestine but do not invade the cells. Therefore, antigiardiasis drugs need not cross the intestinal epithelial burier. Chemical modifications of disulfiram that minimize absorption through the gut but still enable transport into the trophozoites will further reduce the risks of off target inhibition and side effects.

Because ultimately resistance develops against any drug, the use of combination therapies reduces the rate of emerging resistance. This strategy may be employed in combating the spread of drug resistance in *G. lamblia*. Combination therapy using one of the current standard care drugs with disulfiram would also facilitate dose reduction and therefore the undesirable side effects of drugs such as metronidazole.

Finally, the adult mouse model offers convenience and reduces accidental injuries during oral gavage. The caveat is that no *G. lamblia* strain other than GS has been reported to infect adult mice in the laboratory whereas so far, no *G. lamblia* GS isolate exhibiting metronidazole resistance has been reported. Nonetheless, the new *G. lamblia* axenization method may be applied also to the neonatal mouse model, simplifying the currently used procedure and reducing the number of scarified animals (31) while enabling *in vivo* drug trials against metronidazole-resistant *G. lamblia* isolates.

Acknowledgements—We thank the staff at GM/CA-CAT of the Advanced Photon Source and Dr. Chen Chen for assistance in the x-ray data acquisition. We also thank Dr. Lars Eckmann and Dr. Yukiko Miyamoto for providing the metronidazole-resistant G. lamblia isolate (716 M) and Dr. Theodore Nash for valuable advice about the mouse model.

REFERENCES

1. Ankarklev, J., Jerlström-Hultqvist, J., Ringqvist, E., Troell, K., and Svärd, S. G. (2010) Behind the smile: cell biology and disease mechanisms of *Giardia* species. *Nat. Rev. Microbiol.* **8,** 413–422
2. Cañete, R., Escobedo, A. A., González, M. E., Almirall, P., and Cantelar, N. (2006) A randomized, controlled, open-label trial of a single day of mebendazole *versus* a single dose of tinidazole in the treatment of giardiasis in children. *Curr. Med. Res. Opin.* **22,** 2131–2136
3. Escobedo, A. A., Alvarez, G., González, M. E., Almirall, P., Cañete, R., Cimerman, S., Ruiz, A., and Pérez, R. (2008) The treatment of giardiasis in children: single-dose tinidazole compared with 3 days of nitazoxanide. *Ann. Trop. Med. Parasitol.* **102,** 199–207
4. Lemée, V., Zaharia, I., Nevez, G., Rabodonirina, M., Brasseur, P., Ballet, J. J., and Favennec, L. (2000) Metronidazole and albendazole susceptibility of 11 clinical isolates of *Giardia duodenalis* from France. *J. Antimicrob. Chemother.* **46,** 819–821
5. Upcroft, P., and Upcroft, J. A. (2001) Drug targets and mechanisms of resistance in the anaerobic protozoa. *Clin. Microbiol. Rev.* **14,** 150–164
6. Wensaas, K. A., Langeland, N., and Rortveit, G. (2009) Prevalence of recurring symptoms after infection with *Giardia lamblia* in a non-endemic area. *Scand. J. Prim. Health Care* **27,** 12–17
7. Schofield, P. J., Costello, M., Edwards, M. R., and O'Sullivan, W. J. (1990) The arginine dihydrolase pathway is present in *Giardia intestinalis*. *Int. J. Parasitol.* **20,** 697–699
8. Galkin, A., Kulakova, L., Wu, R., Nash, T. E., Dunaway-Mariano, D., and Herzberg, O. (2010) X-ray structure and characterization of carbamate kinase from human parasite *Giardia lamblia*. *Acta Crystallogr. Sect. F Struct. Biol. Cryst. Commun.* **66,** 386–390
9. Lim, K., Kulakova, L., Galkin, A., and Herzberg, O. (2013) Crystal structures of carbamate kinase from *Giardia lamblia* bound with citric acid and AMP-PNP. *PLoS One* **8,** e64004
10. Chen, C. Z., Southall, N., Galkin, A., Lim, K., Marugan, J. J., Kulakova, L., Shinn, P., van Leer, D., Zheng, W., and Herzberg, O. (2012) A homogenous luminescence assay reveals novel inhibitors for *Giardia lamblia* carbamate kinase. *Curr. Chem. Genomics* **6,** 93–102
11. Chen, C. Z., Kulakova, L., Southall, N., Marugan, J. J., Galkin, A., Austin, C. P., Herzberg, O., and Zheng, W. (2011) High throughput *Giardia lamblia* viability assay using bioluminescent ATP content measurements. *Antimicrob. Agents Chemother.* **55,** 667–675
12. Kitson, T. M. (1983) Mechanism of inactivation of sheep liver cytoplasmic aldehyde dehydrogenase by disulfiram. *Biochem. J.* **213,** 551–554
13. Lipsky, J. J., Shen, M. L., and Naylor, S. (2001) *In vivo* inhibition of aldehyde dehydrogenase by disulfiram. *Chem. Biol. Interact.* **130,** 93–102
14. Fuller, R. K., and Gordis, E. (2004) Does disulfiram have a role in alcoholism treatment today? *Addiction* **99,** 21–24
15. Malcolm, R., Olive, M. F., and Lechner, W. (2008) The safety of disulfiram for the treatment of alcohol and cocaine dependence in randomized clinical trials: guidance for clinical practice. *Expert Opin. Drug Saf.* **7,** 459–472
16. Nash, T., and Rice, W. G. (1998) Efficacies of zinc-finger-active drugs against *Giardia lamblia*. *Antimicrob. Agents Chemother.* **42,** 1488–1492
17. Kabsch, W. (2010) XDS. *Acta Crystallogr. D Biol. Crystallogr.* **66,** 125–132
18. Evans, P. R. (2011) An introduction to data reduction: space-group deter-

mination, scaling and intensity statistics. *Acta Crystallogr. D Biol. Crystallogr.* **67,** 282–292
19. Winn, M. D., Ballard, C. C., Cowtan, K. D., Dodson, E. J., Emsley, P., Evans, P. R., Keegan, R. M., Krissinel, E. B., Leslie, A. G., McCoy, A., McNicholas, S. J., Murshudov, G. N., Pannu, N. S., Potterton, E. A., Powell, H. R., Read, R. J., Vagin, A., and Wilson, K. S. (2011) Overview of the CCP4 suite and current developments. *Acta Crystallogr. D Biol. Crystallogr.* **67,** 235–242
20. Adams, P. D., Grosse-Kunstleve, R. W., Hung, L. W., Ioerger, T. R., McCoy, A. J., Moriarty, N. W., Read, R. J., Sacchettini, J. C., Sauter, N. K., and Terwilliger, T. C. (2002) PHENIX: building new software for automated crystallographic structure determination. *Acta Crystallogr. D Biol. Crystallogr.* **58,** 1948–1954
21. Karle, I. L., Estlin, J. A., and Britts, K. (1967) The crystal and molecular structure of tetraethylthiuram disulfide, $C_{10}N_2H_{20}S_4$. *Acta Crystallogr.* **22,** 273–280
22. Emsley, P., Lohkamp, B., Scott, W. G., and Cowtan, K. (2010) Features and Development of Coot. *Acta Crystallogr. D. Biol. Crystallogr.* **66,** 486–501
23. Bacon, D. J., and Anderson, W. F. (1988) A fast algorithm for rendering space-filling molecule pictures. *J. Mol. Graph.* **6,** 219–220
24. Kraullis, P. J. (1991) A program to produce both detailed and schematic plots of protein structures. *J. Appl. Crystallogr.* **24,** 946–950
25. Nash, T. E., McCutchan, T., Keister, D., Dame, J. B., Conrad, J. D., and Gillin, F. D. (1985) Restriction-endonuclease analysis of DNA from 15 *Giardia* isolates obtained from humans and animals. *J. Infect. Dis.* **152,** 64–73
26. Townson, S. M., Laqua, H., Upcroft, P., Boreham, P. F., and Upcroft, J. A. (1992) Induction of metronidazole and furazolidone resistance in *Giardia*. *Trans. R Soc. Trop. Med. Hyg.* **86,** 521–522
27. Keister, D. B. (1983) Axenic culture of *Giardia lamblia* in TYI-S-33 medium supplemented with bile. *Trans. R Soc. Trop. Med. Hyg.* **77,** 487–488
28. Byrd, L. G., Conrad, J. T., and Nash, T. E. (1994) *Giardia lamblia* infections in adult mice. *Infect Immun.* **62,** 3583–3585
29. Garman, E. F. (2010) Radiation damage in macromolecular crystallography: what is it and why should we care? *Acta Crystallogr. D Biol. Crystallogr.* **66,** 339–351
30. Weik, M., Ravelli, R. B., Kryger, G., McSweeney, S., Raves, M. L., Harel, M., Gros, P., Silman, I., Kroon, J., and Sussman, J. L. (2000) Specific chemical and structural damage to proteins produced by synchrotron radiation. *Proc. Natl. Acad. Sci. U.S.A.* **97,** 623–628
31. Tejman-Yarden, N., Millman, M., Lauwaet, T., Davids, B. J., Gillin, F. D., Dunn, L., Upcroft, J. A., Miyamoto, Y., and Eckmann, L. (2011) Impaired parasite attachment as fitness cost of metronidazole resistance in *Giardia lamblia*. *Antimicrob. Agents Chemother.* **55,** 4643–4651
32. Ramachandran, G. N., Ramakrishnan, C., and Sasisekharan, V. (1963) Stereochemistry of polypeptide chain configurations. *J. Mol. Biol.* **7,** 95–99
33. Laskowski, R. A., MacArthur, M. W., Moss, D. S., and Thornton, J. (1993) PROCHECK: a program to check the stereochemical quality of protein structures. *J. Appl. Crystallogr.* **26,** 283–291